Underestimation of body waves and feasibility of surface-wave reconstruction by seismic interferometry

FARNOUSH FORGHANI and ROEL SNIEDER, Colorado School of Mines

Interferometry is an approach to extract the Green's function between two receivers as if the virtual source is at one of the receiver locations. The Green's function which is the response to an impulsive source, accounts for the wave propagation in the medium between the two receivers. It is commonly thought that Green's function estimates obtained from interferometry accurately represent the full Green's function, but this is not always the case. In fact, the accuracy of the retrieved Green's function, which consists of the surface and body waves, is in practice restricted by the limited distribution of the sources of field fluctuations. We demonstrate the importance of adequate source distribution for the accuracy of the retrieved Green's function, using examples from interferometry applications. In these examples, sources are controlled (as in exploration seismology) or uncontrolled (as in crustal seismology).

Consider a source-receiver distribution where controlled sources are at the surface and receivers are in the interior (Figure 1). Such a scenario is analyzed by Bakulin and Calvert (2004) who apply interferometry to real 4D VSP data recorded in a well, using controlled shots above the well. They obtain a P-wave image superior to that obtained from surface seismic data. Another example of using sources at the surface and receivers in the interior is shown by Mehta et al. (2007), who apply cross-correlation interferometry to Mars ocean-bottom-cable (OBC) data. Using controlled shots near the ocean surface and receivers at the bottom of the ocean, they obtain the body-wave Green's functions.

Consider another distribution where both sources and receivers are at the surface. This distribution is of special interest because it is the most common case in both exploration and crustal seismology. In all studies where sources and receivers are distributed at the surface, an important question regarding the application of interferometry still remains: Can the body waves be satisfactorily extracted by interferometry? Several studies show extracted body waves in this case to be extremely weak (Campillo and Paul, 2003; Dong et al., 2006; Shapiro and Campillo, 2004), although Roux et al. (2005) and Draganov et al. (2009) identify weak body waves as well as the surface waves between two stations when applying interferometry to ambient seismic noise.

We identify the reasons for underestimation of the body waves by interferometry in the case that sources and receivers are at the surface. We can take advantage of the underestimation of the body waves for reconstruction of the surface waves. The reconstructed surface waves can be used for ground-roll suppression in exploration seismology or velocity tomography in both shallow geophysics and crustal seismology. In order to use the extracted surface waves in these applications, it is important to understand to what extent surface waves can be reconstructed by interferometry. Therefore, we study the feasibility of the reconstruction of surface waves (direct as well as scattered surface waves) by interferometry.

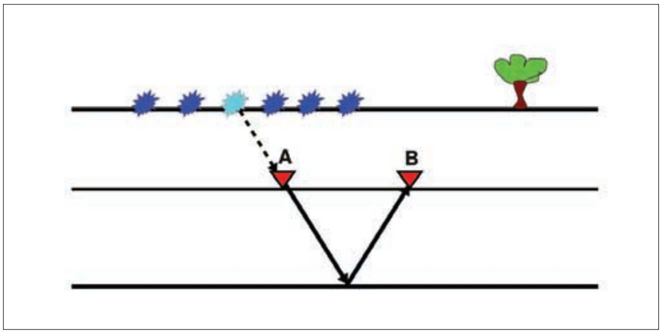

Figure 1. *Illustration of a source-receiver distribution where sources are at the surface and receivers are in the interior. Stars and triangles denote the sources and receivers, respectively. Note that the source in light blue has the largest contribution to the reconstruction of the reflected body-wave between the two receivers.*

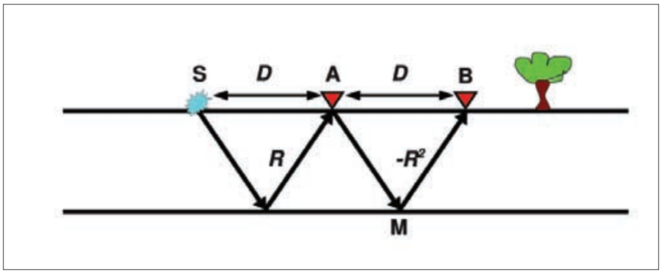

Figure 2. *A two-layer model in a 2D medium; D and R denote the distance and reflection coefficient, respectively.*

Analysis

In the following we present the reasons for the under-representation of the body-wave Green's function by interferometry when both sources and receivers are at the surface. The analysis is corroborated using synthetic examples which are based on a two-layer model in a 2D medium (Figure 2).

Limited number of stationary source locations for body-waves. In Figure 3a, regardless of the source location, cross-correlation of the surface-wave recordings at receivers A and B gives an event with a traveltime that corresponds to the surface wave propagating between A and B (dashed arrow). Therefore, every source location along the source-receiver line on either side of the two receivers contributes to the reconstruction of the surface wave that propagates between the two receivers. For sources between the receivers, however, cross-correlation does not yield the surface wave between A and B.

In contrast to the surface-wave extraction, only specific sources contribute to the retrieval of the body wave propagating between the two receivers. Among all the sources shown in Figure 3b, source *S* contributes most to the extraction of the reflected body wave along raypath AMB. This source, *S*, is the *stationary* source for the reflected body waves. All other sources in dark blue in Figure 3b have a smaller contribution to the reconstruction of the body waves, and are called *nonstationary* sources.

Cross-correlation of the two receiver waveforms from stationary sources yields the correct arrival time for the reflected body waves between the two receivers. However, cross-correlation from nonstationary sources gives an arrival time that does not correspond to the arrival time of the reflected body wave; such an arrival does not correspond to any physical arrival and is called a *nonphysical* arrival (Snieder et al., 2006). It is common in exploration and crustal seismology that few sources are present at the stationary locations.

Small reflection coefficients. To analyze the influence of reflection coefficients on the body-wave amplitude, we consider the two-layer model in Figure 2. We focus on cross-correlating the primary reflection at receiver A with the secondary reflection at receiver B, because the cross-correlation of these two creates the primary reflected body wave propagating along *AMB* between the two receivers. The primary reflection recorded at A has an amplitude proportional to the reflection coefficient R, and the secondary reflection recorded at B has an amplitude proportional to $-R^2$. The negative sign results from the free-surface reflection with reflection coefficient −1.

The above cross-correlation extracts a body-wave that kinematically corresponds to the reflected body wave propagating between the two receivers. The amplitude of the reconstructed body wave is proportional to $-R^3$, while the true amplitude of the reflected body wave between the two receivers is proportional to R. This means that the cross-correlation increases the power of the reflection coefficient and consequently decreases the amplitude of the extracted body wave. For turning waves which have the reflection coefficient R = 1, higher powers of this coefficient do not change the amplitude. Thus, this argument does not apply to turning waves.

Absence of sources under the reflector. Snieder et al. show that adding sources under the reflector can compensate for the amplitude loss of the body waves due to the small reflection coefficients. We summarize their analysis below. As shown in the previous section, for a source at the surface (such as S_1 in Figure 4), the amplitude of the reconstructed body wave between the two receivers is proportional to $-R^3$. On the other hand, the amplitude of the transmitted wave from a source under the reflector (such as S_2) to receiver A is proportional to the transmission coefficient T, and the amplitude at receiver B is proportional to $-TR$. Therefore, the amplitude of the reconstructed body wave from cross-correlating the two receiver waveforms for source S_2 is proportional to $-RT_2$.

In addition to the dependence on the reflection and transmission coefficients, the reconstructed body wave Green's functions from the sources S_1 and S_2 are also proportional to the medium densities above and below the reflector, ρ and ρ_b, respectively. Summing the cross-correlations from the two sources S_1 and S_2 yields the reconstructed body-wave G with the following dependence on R and T:

$$G \propto -(\rho R^3 + \rho_b R T^2) \qquad (1)$$

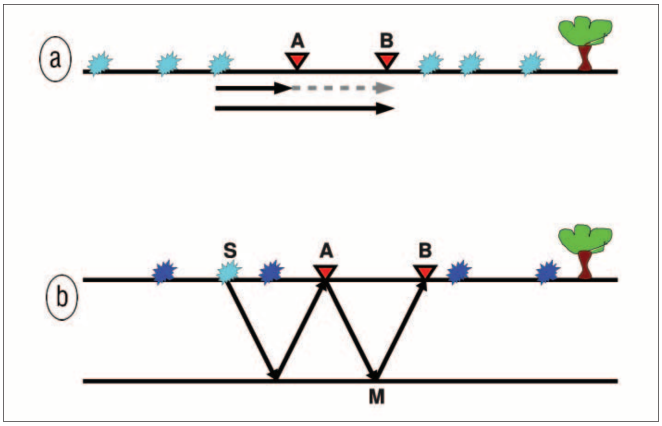

Figure 3. *Source locations that contribute to (a) the surface-wave reconstruction, and (b) the body-wave reconstruction.*

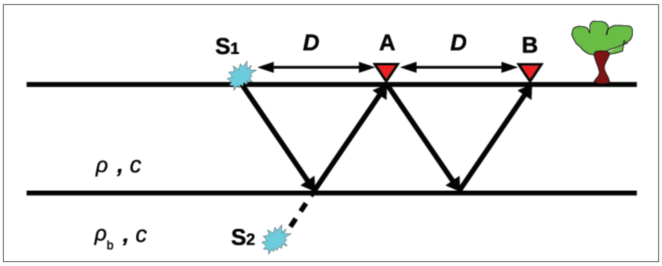

Figure 4. *Sources at the surface and underneath the reflector which give the dominant contribution to the reconstruction of the reflected body-wave between the two receivers.* ρ *and* ρ_b *are the densities of the upper and lower layers, respectively;* c *is the velocity of the two layers.*

Reflection and transmission coefficients for an interface between two layers of equal velocity are given by $R = (\rho_b - \rho) / (\rho_b + \rho)$ and $T = 2\rho / (\rho_b + \rho)$, respectively. Substituting these coefficients into Equation 1 yields

$$G \propto -\rho R \qquad (2)$$

The Green's function in Equation 2 is proportional to R, which is equal to that of the primary reflection between the two receivers. The same analysis can be performed for two layers of different velocities (omitted here for simplicity).

Equation 2 confirms that having sources under the reflector as well as at the surface compensates for the amplitude loss of the body wave caused by a small reflection coefficient. The dominant contribution to the reconstruction of the reflected body wave, G, comes from the two sources S_1 and S_2 (Figure 4). Therefore, the absence of sources under the reflector, a common scenario in crustal seismology with shallow sources as well as in exploration seismology, is another reason for the weak body-wave amplitude extracted by cross-correlation.

Body waves are weak. Geometrical spreading and small reflection coefficients affect the amplitude of the reflected body waves more than the surface waves. This is because of the different propagation paths from source to receiver for these two kinds of waves. Therefore, the recorded reflected body waves are weak compared to the surface waves.

To understand what happens to the amplitude of the body waves after cross-correlation, we illustrate the simplified cross-correlation equation for two waveforms U_A and U_B recorded at receivers A and B in Figure 2, respectively. The waveforms at receivers A and B can be written as $U_A = S_A + B_{RA}$ and $U_B = S_B + B_{RB}$, where S_A and B_{RA} represent the surface and body waves, respectively recorded at receiver A and S_B and B_{RB} are the corresponding waveforms at B. Cross-correlating the two waveforms U_A and U_B which is denoted by C_{AB}, corresponds, in the frequency domain, to

$$C_{AB} = S_B S^*_A + B_{RB} S^*_A + S_B B^*_{RA} + B_{RB} B^*_{RA}. \tag{3}$$

In this equation, the first term denotes the cross-correlation of the surface wave at receiver A with the surface wave at receiver B and gives the surface wave that propagates between the two receivers. The last term, which denotes the cross-correlation of the body wave at receiver A with the body wave at receiver B, is the body wave that propagates between the two receivers. The second and third terms result from the cross-correlation of the body waves with the surface-waves and are called *cross-terms*. These cross-terms do not correspond to any physical arrival and therefore also called nonphysical or *spurious* arrivals.

Equation 3 provides a reason for the weak amplitude of the extracted body-wave Green's function. For most cases, the amplitude of the recorded body wave is substantially smaller than the recorded surface-wave amplitude. After cross-correlation, the amplitude ratio of the body to surface wave is further lowered. Snieder et al. prove that the amplitude loss of the body wave after cross-correlation, which is related to geometrical spreading, can be recovered by integration over the stationary source region. However, recovery of the correct geometrical spreading does not occur in practical situations, where the source distribution near the stationary locations is inadequate.

In Equation 3, for an inadequate source distribution, the cross-terms $B_{RB}S^*_A$ and $S_B B^*_{RA}$ can dominate over the body-wave amplitude. These terms, however, integrate to zero by summing over an adequate number of sources. The cross-term of the body waves with the surface-waves is proportional to $e^{i(k_b r(x) - k_s x)}$, where k_b and k_s are the body-wave and surface-wave wave numbers, respectively; $r(x)$ and x are the travel paths for the reflected body and surface waves from the source to the receiver. Based on the stationary phase approximation, the dominant contribution to the integral with an oscillatory integrand comes from the regions where the phase is stationary and the amplitude varies slowly. Therefore, the integral of the cross-terms, $\int_{-\infty}^{\infty} e^{i(k_b r(x) - k_s x)} dx$, vanishes because the integrand is oscillatory and has no stationary points. The cancellation of these cross-terms is shown by Halliday et al. (2007), where they use a line of sources along the receiver line in a 2D synthetic example.

The synthetic example in Figure 5 shows the cause for the weak body waves reconstructed by Equation 3. For illustration purposes, we set the recorded amplitude ratio of the body to surface-wave ($|B_{RA}/S_A|$ or $|B_{RB}/S_B|$) to approximately 1/2. After cross-correlation of the two receiver waveforms, this ratio becomes about 1/4 (Figure 5c). Note that because

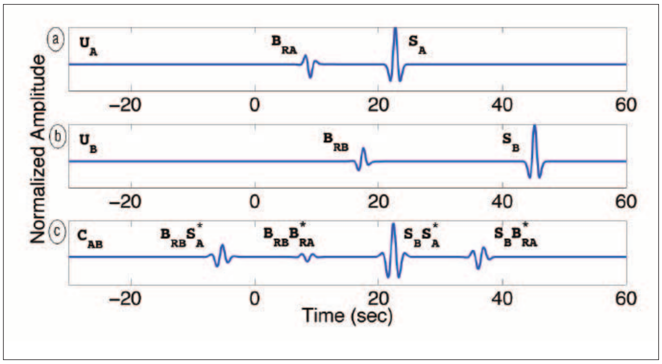

Figure 5. *Loss of the body-wave amplitude by cross-correlation because of the low amplitude ratio of the body to the surface wave: (a) and (b) show the waveforms at receivers A and B, respectively, recorded from source S (in Figure 2);* B_{RA}, S_A, B_{RB} *and* S_B *are the body- and surface-wave terms; (c) shows the cross-correlation of the waveforms in (a) and (b) according to Equation 3.*

we only use one source, the amplitude of the cross-terms is larger than the amplitude of the body wave. When comparing the phase of the body-wave arrivals B_{RA} and B_{RB} in Figures 5a and 5b with the phase of the arrival reconstructed by cross-correlation ($B_{RB}B^*_{RA}$ in Figure 5c), we notice that there is a change in phase between these arrivals. This occurs because only one source contributes to the cross-correlation. Integration over sources at the stationary region, yields a phase shift $\pi / 4$, which accounts for the phase of the body-waves (Snieder et al.).

Application

When sources and receivers are at the surface, the body waves extracted by interferometry are extremely weak and thus the surface waves are dominant. This underestimation of the body waves extracted by interferometry can therefore be exploited to isolate the surface waves which can then be used in ground-roll suppression.

Conventional techniques for ground-roll suppression such as stacking over geophone arrays, polarization methods, and *f-k* filtering, can be used to suppress the direct surface-waves. These techniques are, however, less effective for the suppression of scattered surface-waves (Herman and Perkins, 2006). Recently, interferometry has been used as one alternative for ground-roll suppression (Dong et al., 2006; Halliday et al., 2008, 2007; Vasconcelos et al., 2008). Although interferometry has shown promise in the removal of direct surface waves, its application to the suppression of the scattered surface waves has not been shown. For this reason, it is important to understand to what extent the scattered surface waves can be reconstructed by interferometry.

In this section, we study the feasibility of the surface-wave reconstruction by applying interferometry to the synthetic data from a 3D scattering medium. In our synthetic model, we do not include the body waves; hence, we focus on the dimensions of the surface-wave propagation paths (2D). Our modeling is based on single scattering for isotropic point scatterers (Groenenboom and Snieder, 1995). The phase velocity model used for the surface-wave dispersion (Figure 6) corre-

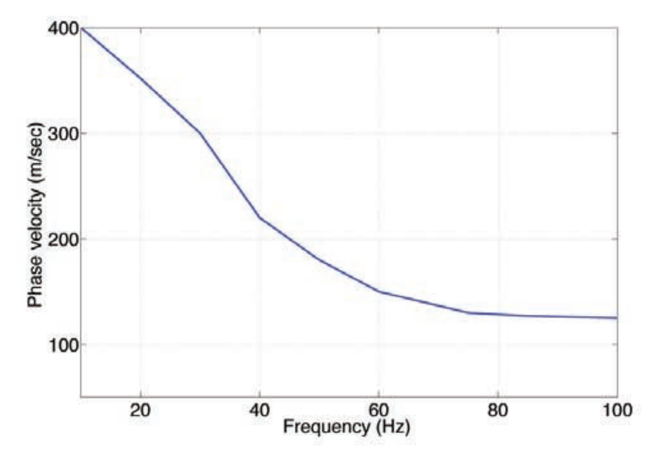

Figure 6. *Surface-wave phase velocity dispersion curve used in the synthetic model.*

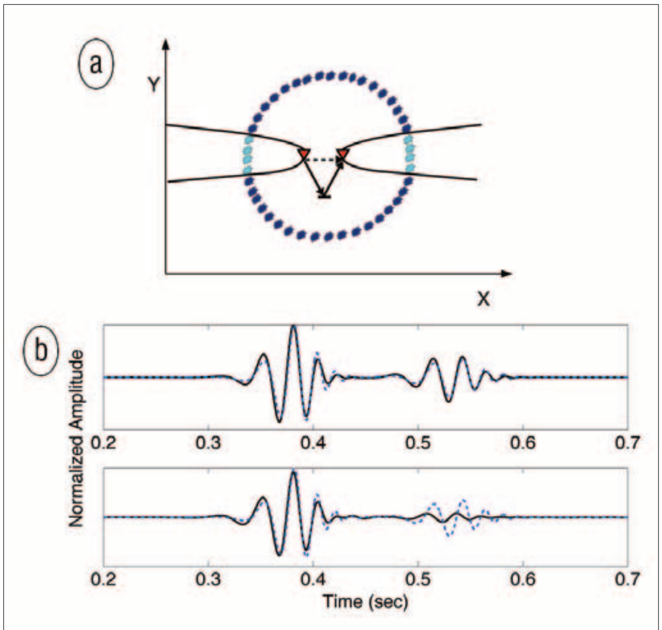

Figure 7. *(a) Plan view of the required sources (light blue) for the reconstruction of the direct surface waves in a 3D medium. (b) Reconstruction of both direct and scattered surface waves (the solid line in the top panel) by summing over all the sources on the closed surface; reconstruction of the direct surface waves (solid line in the bottom panel) by summing over sources in light blue. The waveform shown by the blue dashed line is the direct recorded Green's function at one receiver from a source at the other receiver's location. The first and second arrivals are the direct and scattered surface waves, respectively.*

sponds to the dispersion curves of Luo et al. (2008).

For a 3D medium, if sources of equal power spectrum surround the receivers and the scatterer on all sides (Figure 7a), both direct and scattered surface waves would be reconstructed. As long as sources are present in the vicinity of the receiver line (light blue in Figure 7a), direct surface waves can be reconstructed by interferometry. These light blue sources are the stationary sources for the direct surface waves.

The influence of the source aperture on the reconstruction of the direct surface waves in a 3D medium is illustrated in Figure 7b. Summation of the cross-correlation over all the sources in Figure 7a results in a proper extraction of both the direct and scattered surface waves (upper panel in Figure 7b). Summation over only the light blue sources in Figure 7a, however, reconstructs the direct wave; the reconstructed scattered surface wave has neither the correct amplitude nor the right phase (lower panel in Figure 7b). This is because the stationary source region for the direct surface waves differs from that of the scattered surface-waves.

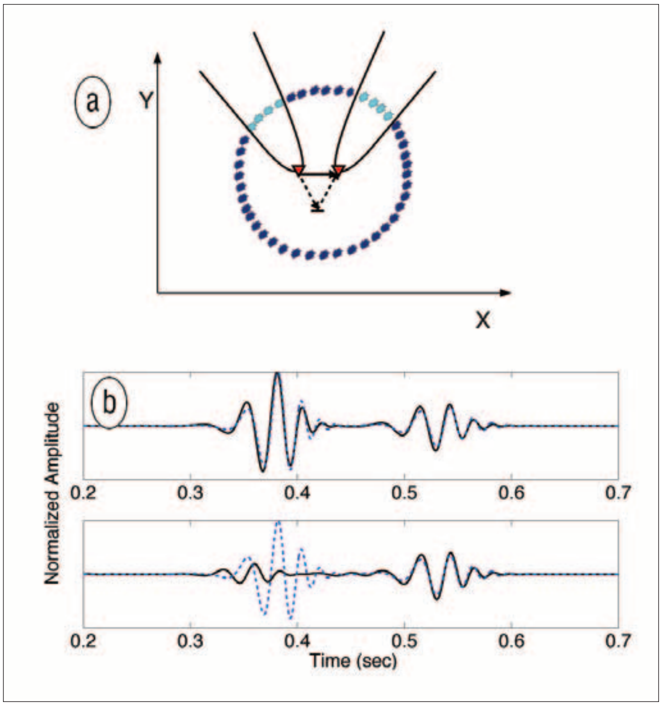

Figure 8. *(a) Plan view of the required sources (light blue) for the reconstruction of the scattered surface waves in a 3D medium. (b) Reconstruction of both direct and scattered surface waves (solid line in the top panel) by summing over all the sources on the closed surface; reconstruction of the scattered surface waves (solid line in the bottom panel) by summing over light blue sources. The waveform shown by the blue dashed line is the direct recorded Green's function at one receiver from a source at the other receiver's location.*

For the reconstruction of the scattered surface-waves, different source positions are needed, depending on the scatterer's location. For the specific location of the scatterer in Figure 8a, the sources in light blue are needed to reconstruct the scattered surface waves. These light blue sources are the stationary sources for the scattered surface waves.

The importance of the source aperture in the reconstruction of the scattered surface wave is evident from Figure 8b. When all sources are included, both direct and scattered surface waves are well reconstructed (same as the upper panel in Figure 7b). However, summation over only the sources in the stationary region for the scattered waves results in their proper reconstruction; the direct waves, on the other hand, show improper extraction (lower panel in Figure 8b).

As mentioned above, the source aperture needed for the reconstruction of the scattered surface waves depends on the location of the scatterer in a medium. Therefore, when the scatterers are distributed throughout the medium, a proper reconstruction of the scattered surface waves necessitates the presence of sources everywhere on the closed surface. This is a much more stringent condition than having sources at the stationary region for the direct waves. For this reason, the extraction of scattered surface-waves by interferometry is more challenging than extracting only direct surface waves.

Conclusions

Studies of the extraction of the Green's function from cross-correlation, when both sources and receivers are at the surface, face a common problem: the underestimation of the body waves compared to the surface waves. We identified the following causes for this problem using analytical reasoning supported by numerical examples:

1) Theory states that for an ideal source distribution on a closed surface surrounding the receivers with sources of the same power spectrum, the exact Green's function between the two receivers can be extracted by cross-correlation. The inability to extract the exact Green's function must therefore be caused by imperfections in the source distribution.

2) For the reconstruction of the direct surface wave, it is sufficient to have a source anywhere along the receiver line as long as it is not between the receivers. For the reconstruction of the body waves, however, the source must be at the appropriate stationary phase region. This condition may not be satisfied by natural or cultural passive sources or even by active sources present in a seismic survey.

3) Cross-correlation of body waves excited by sources at the surface contains a product of reflected waves, which makes their amplitude smaller than the true reflected body waves. Sources at depth can result in a proper reconstruction of the body-wave amplitude; however, since it is uncommon to have controlled sources in the subsurface, the extracted body-wave amplitude remains underestimated.

4) The cross-terms between body waves and surface waves that occur in the cross-correlation for an individual source are much larger than the correlation of the body waves with themselves. These spurious cross-terms between body waves and surface waves integrate to zero when sources are uniformly distributed over a closed surface; but this is not necessarily the case when the distribution of those sources is inhomogeneous.

The underestimation of the body waves from interferometry could potentially be used for surface-wave isolation which in turn is useful for near-surface velocity tomography and ground-roll suppression. Since conventional ground-roll suppression techniques (such as *f-k* filtering) are inadequate for the removal of scattered surface waves, interferometry can possibly provide a proper alternative for suppressing these scattered waves. We studied the feasibility of the surface-wave reconstruction by applying interferometry to the data from a scattering medium. Our analysis shows that one can extract the direct surface waves when sources are present along the receiver line. The extraction of the scattered surface waves is more challenging because the extraction of each of these waves requires sources with an equal strength in each stationary phase region of the scatterer involved. This implies that when scattered waves arrive from all directions (i.e., when scatterers are everywhere), one needs a homogeneous source distribution. This requirement is often not satisfied. TLE

References

Bakulin, A. and R. Calvert, 2004, Virtual source: new method for imaging and 4D below complex overburden: 74th Annual International Meeting, SEG, Expanded Abstracts, 112–115.

Campillo, M. and A. Paul, 2003, Long-range correlations in the diffuse seismic coda: Science, **299**, 547–549.

Dong, S., R. He, and G. Schuster, 2006, Interferometric prediction and least squares subtraction of surface waves: 76th Annual International Meeting, SEG, Expanded Abstracts, 2783–2786.

Draganov, D., X. Campman, J. Thorbecke, A. Verdel, and K. Wapenaar, 2009, Reflection images from ambient seismic noise: Geophysics, **74**, no. 5, A63–A67.

Groenenboom, J. and R. Snieder, 1995, Attenuation, dispersion, and anisotropy by multiple scattering of transmitted waves through distribution of scatterers: Journal of the Acoustical Society of America, **98**, 3482–3492.

Halliday, D., A. Curtis, and E. Kragh, 2008, Seismic surface-waves in a suburban environment: The Leading Edge, **27**, 210–218.

Halliday, D., A. Curtis, J. Robertsson, and D.-J. Manen, 2007, Interferometric surface-wave isolation and removal: Geophysics, **72**, no. 5, A69–A73.

Herman, G. and C. Perkins, 2006, Predictive removal of scattered noise: Geophysics, **71**, no. 2, V42–V49.

Luo, Y., Y. Xu, Q. Liu, and J. Xia, 2008, Rayleigh-wave dispersive energy imaging and mode separating by high-resolution linear Radon transform: The Leading Edge, **27**, 1536–1542.

Mehta, K., A. Bakulin, J. Sheiman, R. Calvert, and R. Snieder, 2007, Improving the virtual source method by wavefield separation: Geophysics, **72**, no. 4, V79–V86.

Roux, P., K. Sabra, B. Grestoft, W. Kuperman, and M. Fehler, 2005, P-wave from cross-correlation of seismic noise: Geophysical Research Letters, **32**.

Shapiro, M. and M. Campillo, 2004, Emergence of broadband Rayleigh waves from correlations of the ambient seismic noise: Geophysical Research Letteres, 31.

Snieder, R., K. Wapenaar, and K. Larner, 2006, Spurious multiples in seismic interferometry of primaries: Geophysics, **71**, no. 4, SI111–SI114.

Vasconcelos, I., J. Gaiser, A. Calvert, and C. Galderon-Macias, 2007, Retrieval and suppression of surface waves using interferometry by correlation and by deconvolution: 77th Annual International Meeting, SEG, Expanded Abstracts, 2566–2570.

Acknowledgments: We are grateful to the National Science Foundation for the financial support through grant EPS-0609595. We are especially thankful to Jyoti Behura for all his helpful discussion, suggestions, and corrections. We also thank Steve Smith, Evert Slob, Seth Hanes, John Stockwell, and Francesco Perrone for suggestions which helped improve this paper.

Corresponding author: fforghan@mymail.mines.edu